HHS Public Access

Author manuscript

Cancer Discov. Author manuscript; available in PMC 2021 August 31.

Published in final edited form as:

Cancer Discov. 2021 June ; 11(6): 1454–1467. doi:10.1158/2159-8290.CD-20-1050.

Mutations in the RAS/MAPK Pathway Drive Replication Repair–Deficient Hypermutated Tumors and Confer Sensitivity to MEK Inhibition

Brittany B. Campbell[#1,2], **Melissa A. Galati**[#1,2], **Simone C. Stone**[3], **Alexandra N. Riemenschneider**[2,4], **Melissa Edwards**[1,2], **Sumedha Sudhaman**[1,2,3], **Robert Siddaway**[2,5], **Martin Komosa**[1,2], **Nuno M. Nunes**[1,2], **Liana Nobre**[1,2], **A. Sorana Morrissy**[6], **Matthew Zatzman**[1,7], **Michal Zapotocky**[2,8,9], **Lazar Joksimovic**[1,2], **Sangeetha N. Kalimuthu**[10], **David Samuel**[11], **Gary Mason**[12], **Eric Bouffet**[8], **Daniel A. Morgenstern**[8], **Melyssa Aronson**[13], **Carol Durno**[13], **David Malkin**[1,8], **John M. Maris**[14], **Michael D. Taylor**[2,4,15], **Adam Shlien**[1,7], **Trevor J. Pugh**[3,16,17], **Pamela S. Ohashi**[3,18], **Cynthia E. Hawkins**[2,5,7], **Uri Tabori**[1,2,3]

[1]Program in Genetics and Genome Biology, The Hospital for Sick Children, Toronto, Ontario, Canada.

[2]The Arthur and Sonia Labatt Brain Tumour Research Centre, The Hospital for Sick Children, Toronto, Ontario, Canada.

[3]Princess Margaret Cancer Centre, University Health Network, Toronto, Ontario, Canada.

[4]Developmental and Stem Cell Biology Program, The Hospital for Sick Children, Toronto, Ontario, Canada.

[5]Program in Cell Biology, The Hospital for Sick Children, Toronto, Ontario, Canada.

Corresponding Author: Uri Tabori, The Hospital for Sick Children, 555 University Avenue, Toronto, Ontario M5G1X8, Canada. Phone: 416-813-7654, ext. 201503; Fax: 416-813-5327; uri.tabori@sickkids.ca.

Authors' Contributions

B.B. Campbell: Conceptualization, data curation, formal analysis, investigation, visualization, methodology, writing–original draft, writing–review and editing. **L. Nobre:** Formal analysis, investigation, methodology, writing–review and editing. **A. Morrissy:** Data curation, formal analysis, investigation, methodology, writing–review and editing. **M. Zatzman:** Resources, data curation, formal analysis, writing–review and editing. **M. Zapotocky:** Resources, data curation, formal analysis, writing–review and editing. **L. Joksimovic:** Resources, data curation, formal analysis, writing–review and editing. **S.N. Kalimuthu:** Resources, data curation, writing–review and editing. **D. Samuel:** Resources, data curation, investigation, writing–review and editing. **G. Mason:** Data curation, investigation, writing–review and editing. **E. Bouffet:** Data curation, supervision, investigation, writing–review and editing. **D.A. Morgenstern:** Data curation, supervision, investigation, writing–review and editing. **M.A. Galati:** Conceptualization, data curation, formal analysis, investigation, visualization, methodology, writing–original draft, writing–review and editing. **M. Aronson:** Data curation, investigation, writing–review and editing. **C. Durno:** Data curation, investigation, writing–review and editing. **D. Malkin:** Data curation, supervision, investigation, writing–review and editing. **J.M. Maris:** Resources, data curation, supervision, investigation, writing–review and editing. **M.D. Taylor:** Resources, data curation, writing–review and editing. **A. Shlien:** Resources, data curation, supervision, investigation, writing–review and editing. **T.J. Pugh:** Resources, data curation, supervision, investigation, writing–review and editing. **P.S. Ohashi:** Data curation, supervision, investigation, writing–review and editing. **C.E. Hawkins:** Resources, data curation, supervision, investigation, writing–review and editing. **U. Tabori:** Conceptualization, resources, data curation, supervision, funding acquisition, investigation, writing–original draft, writing–review and editing. **S.C. Stone:** Conceptualization, data curation, formal analysis, investigation, visualization, methodology, writing–original draft, writing–review and editing. **A.N. Riemenschneider:** Formal analysis, investigation, visualization, methodology, writing–original draft, writing–review and editing. **M. Edwards:** Resources, data curation, investigation, visualization, methodology, writing–original draft, project administration, writing–review and editing. **S. Sudhaman:** Resources, data curation, writing–original draft, project administration, writing–review and editing. **R. Siddaway:** Resources, data curation, formal analysis, writing–review and editing. **M. Komosa:** Resources, data curation, formal analysis, investigation, methodology, writing–review and editing. **N.M. Nunes:** Investigation and methodology.

Authors' Disclosures

No disclosures were reported by the other authors.

Note: Supplementary data for this article are available at Cancer Discovery Online (http://cancerdiscovery.aacrjournals.org/).

[6]Charbonneau Cancer Institute, University of Calgary, Calgary, Alberta, Canada.

[7]Department of Laboratory Medicine and Pathobiology, Faculty of Medicine, University of Toronto, Toronto, Ontario, Canada.

[8]Division of Hematology/Oncology, The Hospital for Sick Children, Department of Pediatrics, University of Toronto, Toronto, Ontario, Canada.

[9]Second Faculty of Medicine, Charles University and University Hospital Motol, Prague, Czech Republic.

[10]Department of Pathology, Laboratory Medicine Program, University Health Network and University of Toronto, Toronto, Ontario, Canada.

[11]Department of Hematology–Oncology, Valley Children's Hospital, Madera, California.

[12]Department of Pediatric Hematology–Oncology, Children's Hospital of Pittsburgh of UPMC, Pittsburgh, Pennsylvania.

[13]Zane Cohen Centre for Digestive Diseases, Mount Sinai Hospital, Toronto, Ontario, Canada.

[14]Division of Oncology and Center for Childhood Cancer Research, Children's Hospital of Philadelphia, and Perelman School of Medicine at the University of Pennsylvania, Philadelphia, Pennsylvania.

[15]Division of Neurosurgery, The Hospital for Sick Children, Toronto, Ontario, Canada.

[16]Department of Medical Biophysics, University of Toronto, Toronto, Ontario, Canada.

[17]Ontario Institute for Cancer Research, Toronto, Ontario, Canada.

[18]Department of Immunology, University of Toronto, Toronto, Ontario, Canada.

[#] These authors contributed equally to this work.

Abstract

The RAS/MAPK pathway is an emerging targeted pathway across a spectrum of both adult and pediatric cancers. Typically, this is associated with a single, well-characterized point mutation in an oncogene. Hypermutant tumors that harbor many somatic mutations may obscure the interpretation of such targetable genomic events. We find that replication repair–deficient (RRD) cancers, which are universally hypermutant and affect children born with RRD cancer predisposition, are enriched for *RAS/MAPK* mutations ($P = 10^{-8}$). These mutations are not random, exist in subclones, and increase in allelic frequency over time. The RAS/MAPK pathway is activated both transcriptionally and at the protein level in patient-derived RRD tumors, and these tumors responded to MEK inhibition *in vitro* and *in vivo*. Treatment of patients with RAS/MAPK hypermutant gliomas reveals durable responses to MEK inhibition. Our observations suggest that hypermutant tumors may be addicted to oncogenic pathways, resulting in favorable response to targeted therapies.

INTRODUCTION

Tumor hypermutation is defined by an excess of somatic mutations (>10 mut/Mb). On the basis of this definition, nearly one fifth of human cancers are hypermutated, and nearly all tissue types have a subset of tumors that are hypermutated (1–3). Multiple reports have concluded that hypermutant tumors are unique in their evolution, are resistant to conventional chemotherapies, and confer poor patient survival (4, 5).

Hypermutation arises as a result of various underlying processes (6). These include environmental exposures (UV radiation, refs. 7, 8; smoking, ref. 9; aristolochic acid exposure, ref. 10), chemotherapy (alkylators; ref. 11), and replication repair deficiency (RRD), among others.

Mutations arising from replication repair–related errors have been causally implicated in two-thirds of human cancers (12, 13). RRD and associated hypermutation can result from germline or somatic mutations in either DNA polymerases *(POLE* and *POLD1*; ref. 14) or in the mismatch-repair genes (*MSH2, MSH6, MLH1*, and *PMS2*; ref. 15). Furthermore, germline biallelic loss of any of the mismatch-repair genes results in one of the most aggressive human cancer syndromes, termed constitutional mismatch-repair deficiency syndrome (CMMRD). These patients develop cancers in numerous organs during childhood and harbor the highest mutation burden (>300 mutations/MB) of any human cancer type (16). Due to the tumor burden and their inherent resistance to conventional therapies, these patients tend to have extremely poor outcomes.

Targeting hypermutated tumors with immune-checkpoint inhibitors results in clinical benefit (17–22). Recent data have demonstrated that in some cancer types, high mutational burden is a strong predictor of response to immune-checkpoint inhibition (23). The PD-1 inhibitor pembrolizumab is now approved for therapy in all RRD cancers, reinforcing the agnostic, mechanism-based indication for a cancer therapeutic (24). However, immune-checkpoint inhibition alone has not been universally effective (25–27). Defining other vulnerabilities of hypermutant cancers is a major aim of the cancer research community.

Single-nucleotide alterations in proto-oncogenes that regulate cell growth and proliferation pathways are a commonly observed tumor-promoting event (28). One such pathway is the well-characterized RAS/MAPK pathway, where gain-of-function mutations in *RAS* and/or downstream effectors result in constitutive dysregulation of signaling to upregulate transcription factors involved in diverse cellular processes conferring survival advantage. Although canonical amino acid changes, such as a valine to glutamic acid at position 600 in $BRAF^{V600E}$, or a glycine to aspartic acid substitution at position 12 in $KRAS^{G12D}$, are commonly observed in multiple cancers (29), the spectrum of potentially actionable RAS/MAPK activating mutations in hypermutated cancers and whether these mutations are actively selected in the context of RRD-derived hypermutation is largely unknown.

Importantly, recent reports have noted that nonsynonymous mutations in RAS/MAPK pathway genes (i.e., *HRAS, NRAS*, and *BRAF*) exhibit strong selection, regardless of their amino acid position (30). In addition, mutations in RAS/MAPK signaling members downstream of the typical receptor tyrosine kinases, such as *MAPK1, MAP2K1, MAP2K2,*

MAP2K4, and *MAP3K13*, have been found to be significantly more frequently mutated than expected by chance by genomic analyses of large tumor data sets of diverse types (31). Thus, the diversity of RAS/MAPK pathway driver mutations, and the genes in which they arise, may be larger than previously anticipated.

Because RAS/MAPK pathway genes are commonly mutated in several childhood cancers, including cancer types commonly associated with CMMRD, we reasoned that hypermutated RRD tumors will harbor functionally impactful mutations in key genes of the RAS/MAPK signaling pathway and therefore would be amenable to RAS/MAPK pathway inhibition.

Here we show that *RAS/MAPK* mutations are enriched in RRD hypermutated tumors and result in activation of the pathway. Treatment of patients with RRD cancers reveals encouraging responses in heavily pretreated children with otherwise poor prognoses.

RESULTS

Mutations in the RAS/MAPK Pathway Are Common in Hypermutated Childhood Cancers

First, to determine the prevalence of *RAS/MAPK* mutations in pediatric cancers, we analyzed all single-nucleotide mutations resulting in nonsynonymous amino acid changes in a large cohort of 1,215 pediatric patients with cancer (ages 0–18; 55% male, 45% female) using targeted sequencing of >400 well-defined cancer genes, sequenced and made publicly available by Foundation Medicine (32). Major tumor subtypes within this cohort consisted of brain tumors, hematologic malignancies, extracranial embryonal tumors, sarcomas, and carcinomas (Fig. 1A; Supplementary Fig. S1). Further information on these tumors and their specific genetic alterations can be found in Supplementary Fig. S1 and Supplementary Table S1. Nonsynonymous mutations in *NRAS, NF1*, and *KRAS* were the second, third, and fourth most common alterations observed following *TP53* across cancers of all types (Fig. 1A). The negative RAS/MAPK pathway regulator *NF1* showed predominantly truncating point mutations, whereas point mutations in oncogenes *NRAS, KRAS, BRAF*, and *PTNP11* were almost exclusively missense (Supplementary Fig. S2). Of the 15 most common genes harboring single-nucleotide variants (SNV) in these childhood cancers, five were RAS/MAPK pathway members, affecting 18% (218/1215) of all childhood tumors. These mutations were observed across most childhood cancers, suggesting that the potential for RAS/MAPK pathway inhibition in pediatric cancer as a therapeutic option may be underexplored.

We then considered hypermutated tumors. These cancers are commonly devoid of copy-number alterations and are characterized by a preponderance of SNVs (16). We observed different RAS/MAPK pathway mutation enrichment among tumor types, suggesting that these mutations are not simply a by-product of hypermutation. First, the prevalence of RAS/MAPK mutations was most commonly observed in gastrointestinal tract cancers and gliomas followed by hematopoietic malignancies (Fisher exact test, $P < 0.0001$). These cancers are associated with the cancer predisposition syndrome CMMRD (33) and therefore driven by RRD. Second, RAS/MAPK mutations were enriched in tumor types known to harbor these alterations regardless of their tumor mutational burden. For example, 60% of hypermutant neuroblastoma harbored mutations in RAS/MAPK genes, consistent

with recent reports (34), whereas hypermutated Wilms tumors and rhabdomyosarcomas rarely harbored mutations in the pathway (Fig. 1B). Third, specific genes in the pathway dominated each respective tumor type. *KRAS* mutations were dominant in gastrointestinal tumors, whereas *NF1* mutations were more dominant in brain tumors (Fig. 1C). This tissue-of-origin selectivity was further supported by comparing central nervous system (CNS) versus colorectal cancers for *NF1* mutations versus *KRAS* dominance in cBioPortal (Supplementary Fig. S3A and S3B). These data support the notion that alterations in the RAS/MAPK pathway in hypermutated cancers are beyond what would be expected by chance and may confer a selective advantage to hypermutated cancer cells.

RRD Cancers Activate the RAS/MAPK Pathway

To further explore the role of RAS/MAPK mutations in RRD hypermutant gliomas and gastrointestinal cancers, we performed high cage exome sequencing (~98×) of 46 tumors from the International RRD consortium (IRRDC), an international group of clinicians and medical scientists studying and treating children and young adults with RRD cancers. Matched controls were obtained and sequenced for all but 2 of 46 tumors (D291_2 and X12). All 46 cancers harbored several point mutations in diverse members of the RAS/MAPK pathway (Fig. 1D; Supplementary Table S2). These included at least one loss-of-function *NF1* mutation in 95% (39/41) of gliomas and often additional missense mutations in intermediary RAS/MAPK pathway members (*MAPK1, MAP2K1, MAP2K2, MAP3K1*, and *MAP3K2*).

Clonal heterogeneity is a major contributor to acquired resistance to current targeted therapies. We anticipated that this may also be a concern in RRD cancers due to their ongoing mutation accumulation and highly polyclonal nature. To determine whether RAS/MAPK mutations exist in different cloverones within RRD cancers, we performed high-resolution subclonal analysis of hypermutated cancers that were sequenced to a mean depth of 750×. We confirmed that every clone in polyclonal tumors contained a nonsynonymous mutation in a RAS/MAPK pathway gene (Fig. 2A). For additional support, we used the variant impact prediction software PolyPhen-2 to confirm that the mutations that arose were predicted damaging in the case of negative regulators, whereas positive regulator genes preferred benign/activating mutations. As observed in general hypermutant childhood cancers, RRD gliomas demonstrated multiple truncating mutations in *NF1*, whereas colorectal tumors preferred activating mutations in tyrosine protein kinase receptors (Fig. 2A).

To determine whether RAS/MAPK mutations persist during clonal evolution of RRD cancers, we established serial xenografts of a hypermutant (20 mutations/MB) colorectal cancer surgically resected from a patient with a homozygous germline *MLH1* mutation. The primary tumor contained one activating mutation in *MAP3K1*, which persisted as a consistently expanding variant allele fraction (VAF) throughout the serial engrafting (Fig. 2B). Two additional RAS/MAPK pathway–activating mutations in *KRAS* and *MAP3K2* arose during serial transplantations and increased from a low to a high VAF, suggesting enrichment for these mutations (Fig. 2B). This enrichment in RAS/MAPK mutations in progressive clones was independent of the original variants in the tumor, which remained

at a stable, clonal VAF between 0.4 and 0.45 across serial xenografts, further suggesting a functional role to these mutations. We conclude that within the RRD cancers, RAS/MAPK mutations are nonrandomly enriched and exist in multiple clones during cancer progression.

Next, we explored whether these mutations result in activation of the RAS/MAPK pathway that can be observed at the transcriptional and translational level. First, we sequenced the full transcriptome of 21 RRD hypermutant glioblastomas that had undergone exome sequencing and harbored confirmed RAS/MAPK pathway alterations (Fig. 1D; Supplementary Table S2), and compared them to five normal adult brain and four normal fetal brain samples. After confirming that global transcriptional patterns between tumor and normal were distinct (Supplementary Fig. S4A), we used several pathway signature models to assess RAS/MAPK pathway activation. We assessed MAPK pathway activity using the signature-based model PROGENy (35), which derives signatures using 100 responsive genes that are most consistently deregulated as a result of MAPK activation. RRD tumors had significantly higher MAPK signature scores than normal samples (Fig. 3A) and distinctly clustered from normals based on the transcriptional output of the PROGENy MAPK pathway genes (Supplementary Fig. S4B). This was not true for housekeeping genes (Supplementary Fig. S4C), suggesting that such clustering does not occur randomly. Using the same RNA sequencing (RNA-seq) data, we could additionally distinctly cluster samples using a gene-expression RAS pathway signature comprised of 18 genes (ref. 36; Fig. 3B). Finally, we performed gene set enrichment analysis (GSEA) of the hallmark gene set for genes upregulated by KRAS activation (37) and found that RRD tumors are significantly enriched for KRAS upregulated genes compared with normal adult and fetal brains [Fig. 3C; normalized enrichment score (NES) = 3.13].

To further directly measure pathway activation, we used a multiplexed RNA and protein detection strategy in which multiple RAS/MAPK pathway–related mRNA and downstream proteins and their phosphorylation are probed and counted directly without previous amplification (NanoString nCounter gene-expression system). RRD hypermutant gliomas had significantly higher expression of genes in the pathway when compared with normal brain ($P = 0.0002$; Fig. 3D). This correlated well with other childhood gliomas with known driver mutations in *NF1, BRAF*^{V600E}, and *BRAF–KIAA1549* fusion, which are known to harbor RAS/MAPK pathway activation and respond well to MEK inhibitors (Fig. 3D). Further examination of the pathway activation using NanoString revealed that RRD hypermutant cancers preferentially expressed high levels of downstream target transcription factors (*FOS, JUN, MYC*) and less of membrane receptors, further supporting the role of mutations in mid-pathway tyrosine kinases which result in activation of the effector genes and a possible loop repression of receptor expression (Fig. 3E).

Activation of RAS/MAPK kinases was also observed at the protein level when comparing phospho-ERK to total ERK and phospho-CRAF in RRD hypermutant gliomas and normal brain using NanoString. RRD gliomas harbored comparable levels of these phosphorylated targets to gliomas driven by *BRAF* and *NF1* alterations (Fig. 3F). As a further confirmation of the assay, protein expression of Ki67 and p53 was significantly higher in RRD high-grade gliomas as compared with low-grade gliomas harboring RAS/MAPK alterations (Fig. 3F), indicating that the increase in phosphorylation observed was not random. Lastly, IHC

staining for phosphor-ERK was performed on 11 hypermutant high-grade glioma and two colorectal cancers in children with germline mutations in replication repair genes (MMR, *POLE*), and 100% of tumors displayed strong positive phospho-ERK staining (Fig. 3G; Supplementary Fig. S5). These data further suggest that RRD hypermutant cancers are driven, in part, by non-random mutations resulting in growth factor receptor–independent activation of the RAS/MAPK pathway.

RRD Hypermutant Cancers Respond to MEK Inhibition

Several RAS/MAPK pathway inhibitors have been developed to block tumor growth driven by this pathway. Those that target the MEK intracellular kinase are already indicated for $BRAF^{V600E}$ melanoma and are currently in various phases of trials for other tumor types, including glioma and colon cancer (38, 39). To test the preclinical benefit of RAS/MAPK inhibitors in RRD hypermutant tumors, we modeled glioma and colon cancers, as these are the tumors most commonly observed in children with RRD. Established colorectal cancer cell lines were first confirmed to be hypermutant and driven by MMR deficiency via signature analysis (COSMIC signatures 6, 14, and 15; Supplementary Fig. S6). Dose-response analysis revealed that both established and patient-derived cells were sensitive to MEK inhibition (Supplementary Fig. S6). We then tested the ability of MEK inhibitors to impede cancer growth *in vivo* using an RRD patient-derived colorectal cancer xenograft with germline *MLH1* mutations (Fig. 4). First, deep sequencing was performed to confirm that the tumor harbored clonal and subclonal RAS/ MAPK mutations (Fig. 4A). Mice injected with patient-derived colorectal cancer cells and treated daily with trametinib demonstrated significantly increased survival benefit (Fig. 4B). Moreover, daily treatment with either MEK inhibitor (selumetinib or trametinib) independently resulted in reduced tumor growth, and significant RAS/MAPK pathway–specific growth arrest as exhibited by decreased phosphorylation of ERK and MEK and increased apoptosis (Fig. 4B and C).

Similarly, use of MEK inhibitors for the treatment of a patient-derived pediatric high-grade glioma with confirmed hypermutation (299 mut/Mb), multiple RAS/MAPK pathway mutations, and a clear RRD signature (Fig. 5A–D) resulted in significant response to both trametinib and selumetinib *in vitro* (Fig. 5E). Moreover, xenografts established from these primary cultures demonstrated improved survival when treated with trametinib ($P = 0.0001$) and reduced tumor growth in response to either inhibitor *in vivo* ($P = 0.0039$; Fig. 5F and G).

Encouraging Responses to MEK Inhibition in Patients with RRD Gliomas

Two patients from the IRRDC who had RAS/MAPK active gliomas were treated with MEK inhibitors. Patient 1, a patient with CMMRD harboring homozygous *PMS2* germline mutations, was diagnosed at age three years with an inoperable diffuse glioma (Fig. 6A). The patient underwent three distinct chemotherapy protocols (combination vincristine plus carboplatin, vinblastine, and temozolomide, respectively) and failed to achieve a measurable response by RECIST criteria (Fig. 6A, left scan). The patient was then treated with selumetinib as a fourth line of treatment, which resulted in the first measurable response (80% reduction in tumor volume) as observed by MRI and three years of stable disease (Fig. 6A, right scan).

Patient 2, a patient with CMMRD harboring homozygous germline *PMS2* mutations, was diagnosed at age 14 years with glioblastoma multiforme (GBM; WHO grade IV). The patient was initially treated with gross total surgical resection and radiation and, upon tumor recurrence, was treated with the anti–PD-1 inhibitor nivolumab. In parallel, molecular analysis of the tumor confirmed ultrahypermutation and multiple RAS/MAPK pathway mutations (Supplementary Fig. S7A). Following multifocal progression on nivolumab alone, addition of trametinib resulted in remarkable resolution of these lesions with maximum response in five months (Fig. 6B). This response persisted for a total of nine months as a third line of therapy for this cancer. To further elucidate the immune response to therapy, we collected serial blood samples and isolated peripheral blood mononuclear cells (PBMC) throughout the duration of nivolumab administration for patient 2. Using flow-cytometric analysis, we observed an increase in proliferating $CD3^+CD8^+$ T cells one month after the addition of trametinib to anti–PD-1 therapy (Fig. 6C and D). These proliferating T cells also expressed the tumor-reactive T-cell marker CD39 (Supplementary Fig. S7B; refs. 40, 41). This increase in proliferation was followed by an increase in the total $CD3^+CD8^+$ T-cell compartment (Fig. 6C) corresponding with tumor regression as observed by MRI (Fig. 6B). Similar increases in proliferating and total $CD3^+CD8^+$ T cells one month after anti–PD-1 initiation were observed in other CMMRD patients with a GBM that responded to anti–PD-1 alone, whereas no changes to the PBMC T-cell compartment were observed in CMMRD patients with a GBM that showed no clinical response to anti–PD-1 treatment (Fig. 6C and D). Collectively, these data further suggest that RRD hypermutant cancers that upregulate the RAS/MAPK pathway are susceptible to MEK inhibition, and the addition of MEK inhibitors to immune-checkpoint blockade may promote an immune-mediated antitumor response.

DISCUSSION

Data presented in this study demonstrate that within the polyclonal nature of hypermutant RRD cancers, multiple mutations in the *RAS/MAPK* pathway are enriched and can coexist, which together renders these tumors susceptible to MEK inhibition. Under these circumstances, our current model of subgrouping tumor types by major driver mutation and targeting the respective pathway will preclude many potential candidates for this type of targeted therapy. The one-mutation-one-drug paradigm, as evidenced by targeting $BRAF^{V600E}$ in melanoma and glioma, may be limited in scope. In the context of hypermutation, a spectrum of mutations may activate the RAS/MAPK pathway, which can collectively be targeted therapeutically.

Although Foundation Medicine data provide a sufficiently large cohort to examine the prevalence of RAS/MAPK alterations across pediatric cancers, these data are derived from sequencing of tumors only without comparative normals, and some mutations reported in *NF1* and *PTPN11* may result from germline predisposition, not an enrichment for somatic events across pediatric cancers. However, pediatric tumors driven by germline mutations in *NF1* and *PTPN11* do not result in hypermutated cancers but rather have extremely low mutational burdens (42). Thus, genetic events in RAS/MAPK genes found in the subset of Foundation Medicine tumors deemed to be hypermutant are likely to be somatic and not germline events.

As we learn more about the emergence, clonal evolution, and progression of RRD-driven hypermutant cancers (43), a different approach is warranted to manage these patients. Novel therapies that rely on a specific target, such as CD19 CAR T-cell and tyrosine kinase inhibitor therapy, may fail as RRD tumors are polyclonal and continuously accumulate mutations, ultimately resulting in loss of the antigen or acquiring resistance to the target, respectively (44).

Dependence of these hypermutant cancers on RAS/MAPK alterations may be explained conceptually by “oncogene addiction,” defined as cancers that contain multiple genetic and chromosomal abnormalities but are dependent on or “addicted” to one or a few mutations for both maintenance of the malignant phenotype and cell survival (39). Moreover, previous studies have demonstrated striking synthetic lethal interactions between MEK inhibitors and inhibitors of other DNA-repair pathways including homologous recombination (45, 46). Our findings provide further support that activation of the RAS/MAPK pathway may synergize with functional DNA-repair elements, which may be required to protect tumor cells undergoing excessive DNA damage. Germline RRD cancers from this study provide a unique opportunity to study synthetic lethal interactions between RRD and MEK inhibition.

Mutations in the MMR and polymerase genes result in a hypermutation phenotype, and the oncogenic mutations that drive these cancers may initially be obscured. A multidimensional analysis, which integrates evidence for pathway activation in the form of multiclonal point mutations (DNA level), gene expression (RNA level), and phospho-protein probing (protein level), provides a strong rationale for therapy targeting a specific pathway even if canonical mutations are not present.

One oft-cited caveat to using targeted therapies is the risk of a tumor not responding completely due to inherent resistance of some clones in the tumor that do not carry the pathway-specific mutation. Our data suggest that RRD cancers invariably harbor mutations in the RAS/MAPK pathway, with unique mutations being observed across subclones (Fig. 2A), and are found to enrich over time (Fig. 2B). Although our observations suggest that activation of the RAS/MAPK oncogenic pathway is a necessary process that governs RRD tumors, additional studies may be needed to further assess tumor dependence on this pathway and whether such addiction is sufficient to overcome the genomic instability of these cancers. Moreover, mechanisms of resistance in RRD tumors that respond and subsequently relapse after treatment with MEK inhibitors are currently unknown. Therefore, combination with other pathway inhibitors or immune-based approaches should be considered.

The second patient in this study was treated with the anti–PD-1 inhibitor nivolumab, currently indicated for MMR-deficient and hypermutant cancers (19, 24, 47). Combinatorial immune-checkpoint inhibitors have been suggested to be the next step in the evolution of immune-based therapies against cancer (48–50). The success of such combinations, however, may be related to the underlying mechanisms driving tumorigenesis and hypermutation (51). Thus, recent data suggesting a lack of response in nonhypermutant colorectal cancers to combined immune-checkpoint inhibition with MEK inhibitors may not be relevant to RRD hypermutant cancers (52). Our data and the encouraging responses in

CMMRD children with RRD hypermutant cancers suggest that a high mutation burden due to RRD may be required to achieve durable clinical benefit; however, clinical trials will be necessary to better assess the efficacy of MEK inhibitors in these patients.

In summary, this study suggests that a nuanced analytic approach to the pattern of pathway-specific mutations that arise in hypermutant cancers can reveal a targetable therapeutic opportunity. Given that hypermutation is observed in up to 20% of cancers at presentation and possibly higher at recurrence, these approaches should be explored in future clinical trials, which are agnostic to tissue of origin and focus on common mechanisms such as hypermutation.

METHODS

Patient and Sample Collection for Exome Sequencing and PBMC Collection

A cohort of germline replication repair–deficient patients with known clinical history was collected as described previously (16). In brief, patients were registered as a part of the International Replication Repair Deficiency Consortium, which includes multiple centers worldwide. The study was conducted in accordance with the Canadian Tri-Council Policy Statement II (TCPS II). Following Institutional Research Ethics Board approval, all data were centralized in the Division of Haematology/Oncology at The Hospital for Sick Children (SickKids). Written, informed consent was obtained from patients' parents or guardians, or from the patients, where applicable. Family history, demographic, and clinical data were obtained from the responsible physician and/or genetic counselor at the corresponding centers.

Targeted Panel Sequencing

FoundationOne panel sequencing was performed on 1,215 pediatric tumors, and variants were shared via the pediatric portal https://pediatric-data.foundationmedicine.com/.

Targeted sequencing was performed as previously described (1). In brief, exonic hybridization capture of >400 genes implicated in cancer was applied to a minimum of 50 ng of DNA extracted from formalin-fixed paraffin-embedded clinical cancer specimens. Pathologic diagnosis of each case was confirmed by review of hematoxylin and eosin–stained slides, and samples were excluded if found to contain <20% tumor cells. Libraries were sequenced to high uniform median coverage (>500×) and assessed for base substitutions, copy-number alterations, and gene fusions/rearrangements.

Whole-Exome Sequencing

High-throughput sequencing, read mapping, and identification of mutations were performed at The Center for Applied Genomics at The Hospital for Sick Children. Tumor and matched blood-derived DNA were run using Agilent's exome enrichment kit (Sure Select V4/V5; with >50% of baits above 25× coverage), on an Illumina HiSeq2500. Base calls and intensities from the Illumina HiSeq 2500 were processed into FASTQ files using CASAVA and/or HAS. The paired-end FASTQ files were aligned to UCSC's hg19 GRCh37 with BWA. Aligned reads were realigned for known insertion/deletion events using SRMA and/or

GATK. Base quality scores were recalibrated using the Genome Analysis Toolkit26 (v1.1–28). Somatic substitutions were identified using MuTect (v1.1.4). Mutations were then filtered against common single-nucleotide polymorphisms (SNP) found in dbSNP (v132), the 1000 Genomes Project (Feb 2012), a 69-sample Complete Genomics data set, and the Exome Sequencing Project (v6500) and the ExAc database.

Subclone Analysis

Tumor subclones were determined using the R package SciClone (53). Specific RAS/MAPK variants specific to each clone were identified following distribution of the variants to their respective subclones.

Variant Impact Prediction Software

Variant Impact prediction was performed using PolyPhen-2 (54), http://genetics.bwh.harvard.edu/pph2/.

RNA-seq

Twenty-one hypermutant pediatric GBMs collected by the RRD consortium underwent stranded, poly-A capture RNA-seq following library preparation using the NEBNext Poly(A) mRNA Magnetic Isolation kit. Raw RNA-seq reads were mapped to the human genome (build hg38) using the STAR aligner (v2.4.2a) in two-pass mode and gene annotations from GENCODE v25. Duplicates were marked and removed with Picard Tools prior to quantification of gene counts. Gene counts were calculated using the python script htseq-count (v0.6.1). Raw counts were normalized with the R package DEseq and pathway activation determined with the R package PROGENy. Differential expression was analyzed with edgeR and preranked GSEA performed on the Hallmarks gene sets after ranking genes according to rankScore = sign(log2FC) × $-\log_{10}$(edgeR-adjusted *P* value).

NanoString Ncounter Gene-Expression System

Total RNA was isolated from 5- to 10-mm scrolls of formalin-fixed paraffin-embedded (FFPE) preserved tissue with the RNeasy FFPE extraction kit (QIAGEN). RNA quantity and quality were assessed using the NanoDrop 2000 (Thermo Scientific). Samples displaying NanoDrop values of 2.0 to 2.1 were utilized.

Five hundred nanograms of total RNA input was used on the NanoString nCounter system (NanoString Technologies).

In Vivo *Serial Xenograft Experiment*

All mouse studies were approved and performed in accordance with the policies and regulations of the Institutional Animal Care Committee of The Hospital for Sick Children in Toronto. Athymic NOD/SCID gamma mice (The Jackson Laboratory) underwent subcutaneous implantation of a 1 × 1 cm piece of a patient-derived RRD hypermutant colorectal tumor and propagated for 90 days. Half of the tumor was then harvested for DNA extraction and exome sequencing, while the second half was implanted into a new mouse. The procedure was repeated three to four times.

In Vivo *Treatment of Patient-Derived Xenografts*

Primary human colorectal and brain pathologic and post-surgical core biopsies were obtained following Institutional Research Ethics Board approval and written informed consent obtained through the IRRDC. 1×10^6 isolated GBM cells were implanted subcutaneously into three groups of ten mice each (vehicle and selumetinib and/or trametinib). Engrafted mice were administered trametinib (1 mg/kg; refs. 55–57) or selumetinib (100 mg/kg; refs. 58–60) via oral gavage daily until endpoint.

Western Blotting

Tissue samples were flash-frozen with liquid nitrogen and then mechanically pulverized to fine powder using a mortar and pestle. Samples were lysed using hot 2× SDS buffer with sodium orthovanidate and phosphoinhibitor cocktails II (Millipore Corp; cat. #524625–1SET) and IV (Calbiochem; cat. #524628–1SET). Protein concentrations were quantified using Thermo Fisher's Pierce BCA protein assay kit (cat. #23227). Equal loading (20 μg protein) was ensured for each blot. Fresh bromophenol blue dye and dithiothreitol (DTT; final concentration 100 mmol/L) were added to lysate aliquots and boiled immediately before resolution. All samples were resolved using SDS-PAGE, 12% bis-acrylamide gels, and transferred using BioRad's semidry transfer system to a PVDF membrane. α-Tubulin was used as a loading control. Membranes were probed with primary antibodies specific to protein of interest: MEK1/2, phospho-MEK1/2, ERK1/2, phospho-ERK1/2, caspase-3, cleaved caspase-3, PARP; α-tubulin, T5168, Sigma. Lysis buffer composition: 2 mL 100% glycerol + 2 mL (10% SDS) + 5.4 mL H_2O + 400 μL 0.5M EDTA + 200 μL 1.0M TRIS + 50 μL protease and phosphoinhibitors.

IHC for RAS/MAPK Pathway Upregulation

Nuclear pERK staining of 11 RRD glioma and two colorectal cancers was performed using phospho-p44/42 MAPK (ERK1/2; Thr202/Tyr204) antibody (Cell Signaling Technology; cat. #9101). All slides were subject to pathologic review. Images were reviewed and captured using the open source software for digital pathology analysis: QuPath.

Cell Lines

Colorectal cancer cell lines HCT116 and HCT15 were purchased from ATCC and certified *Mycoplasma* free (August 2013). Passage 3 from both HCT116 and HCT15 was used for *in vitro* and sequencing experiments. LoVo was obtained from C. Pearson, The Hospital for Sick Children, Toronto, Canada (April 2016) and passage 4 was used for *in vitro* and sequencing experiments. Both LoVo and HCT116 were confirmed *Mycoplasma* free using the PCR Mycoplasma Test Kit; cat. #409010 (mdbiosciences, March 2017). The patient-derived high-grade glioma cell line (Fig. 5) was established in December 2016, passaged 21 times before being used in *in vitro* experiments, and certified *Mycoplasma* free using the Mycoplasma PCR Detection Kit Catalog #G238 (abm; August 2020). Treatments were performed with the MEK inhibitor trametinib (SelleckChem GSK1120212) or selumetinib (SelleckChem AZD6244).

Flow Cytometry

Viable frozen PBMCs were incubated with Fc block (BD Biosciences) prior to staining for surface markers (anti-CD3—clone UCHT1; anti-CD4—clone RPA-T4; anti-CD8—clone RPA-T8; anti-CD39—clone A1; anti-Ki-67—clone 20Raj1) and viability dye (eBioscience). Cells were fixed and permeabilized for intercellular staining with the FOXP3 transcription factor staining buffer set (BD). Flow cytometry voltages were set using Rainbow beads (Spherotech) with the same setting between experiments. Samples were acquired on a BD LSRFortessa flow cytometer and data were analyzed using the FlowJo software.

Statistical Analysis

Statistical analyses were performed using the GraphPad Prism^{v8} software. The log-rank (Mantel–Cox) test was used to analyze the survival difference for *in vivo* mouse experiments. P values <0.05 were determined to be significant. Asterisks denote P values as follows: *, $P < 0.05$; **, $P < 0.01$; ***, $P < 0.001$; ****, $P < 0.0001$.

Data Availability

Existing whole-exome sequencing data have previously been deposited in the European Genome-Phenome Archive under study accession numbers EGAS00001000579 and EGAS00001001112. New whole-exome sequencing and RNA-seq data generated from this study have been deposited in the European Genome-Phenome Archive under study accession number EGAS00001005008. Public data sets used include cBioPortal (https://www.cbioportal.org/). Further information and/or requests for data will be fulfilled by the corresponding author, Uri Tabori (uri.tabori@sickkids.ca).

Supplementary Material

Refer to Web version on PubMed Central for supplementary material.

Acknowledgments

The Tabori lab research is supported by Meagan's Walk (MW-2014–10), b.r.a.i.n.child Canada, LivWise, an Enabling Studies Program grant from BioCanRx–Canada's Immunotherapy Network (a Network Centre of Excellence), a Canadian Institutes for Health Research (CIHR) grant (PJT-156006), and the CIHR Joint Canada–Israel Health Research Program. Both the Tabori and Maris labs were supported by a Stand Up To Cancer–Bristol-Myers Squibb Catalyst Research grant (SU2C-AACR-CT-07-17). Stand Up To Cancer (SU2C) is a division of the Entertainment Industry Foundation. Research grants are administered by the American Association for Cancer Research, the Scientific Partner of SU2C. The Maris lab is also supported by an NCI grant (R35 CA220500). The Hawkins lab was funded by the Government of Canada through Genome Canada and the Ontario Genomics Institute (OGI-171). The Ohashi lab acknowledges support from the Guglietti family through the We Love You Connie Foundation. B.B. Campbell and M.A. Galati were supported by the Government of Ontario. M.A. Galati was supported by The Garron Family Cancer Centre and the Peterborough K.M. Hunter Graduate Program.

G. Mason reports other support from Johnson & Johnson (Janssen) outside the submitted work. E. Bouffet reports grants from Bristol Myers Squibb during the conduct of the study; grants from Roche outside the submitted work. D.A. Morgenstern reports grants from BMS during the conduct of the study; personal fees from Roche, Boehringer-Ingelheim, Bayer, Clarity Pharmaceuticals, ymAbs Therapeutics, and EUSA Pharma outside the submitted work. D. Malkin reports personal fees from Bayer Canada outside the submitted work. T.J. Pugh reports a patent for hybrid-capture sequencing for determining immune cell clonality. C.E. Hawkins reports grants from CIHR and Genome Canada/OGI during the conduct of the study. U. Tabori reports grants from AACR SU2C catalyst BMS supported grant outside the submitted work.

REFERENCES

1. Campbell BB, Light N, Fabrizio D, Zatzman M, Fuligni F, de Borja R, et al.Comprehensive analysis of hypermutation in human cancer. Cell2017;171:1042–56. [PubMed: 29056344]
2. Gargiulo P, Della Pepa C, Berardi S, Califano D, Scala S, Buonaguro L, et al.Tumor genotype and immune microenvironment in POLE-ultramutated and MSI-hypermutated endometrial cancers: new candidates for checkpoint blockade immunotherapy?Cancer Treat Rev2016;48:61–8. [PubMed: 27362548]
3. Pritchard CC, Morrissey C, Kumar A, Zhang X, Smith C, Coleman I, et al.Complex MSH2 and MSH6 mutations in hypermutated microsatellite unstable advanced prostate cancer. Nat Commun2014;5:4988. [PubMed: 25255306]
4. Hunter C, Smith R, Cahill DP, Stephens P, Stevens C, Teague J, et al.A hypermutation phenotype and somatic MSH6 mutations in recurrent human malignant gliomas after alkylator chemotherapy. Cancer Res2006;66:3987–91. [PubMed: 16618716]
5. Touat M, Li YY, Boynton AN, Spurr LF, Iorgulescu JB, Bohrson CL, et al.Mechanisms and therapeutic implications of hypermutation in gliomas. Nature2020;580:517–23. [PubMed: 32322066]
6. Alexandrov LB, Nik-Zainal S, Wedge DC, Aparicio SA, Behjati S, Biankin AV, et al.Signatures of mutational processes in human cancer. Nature2013;500:415–21. [PubMed: 23945592]
7. Cancer Genome Atlas N. Genomic classification of cutaneous melanoma. Cell2015;161:1681–96. [PubMed: 26091043]
8. Pfeifer GP, You YH, Besaratinia A. Mutations induced by ultraviolet light. Mutat Res2005;571:19–31. [PubMed: 15748635]
9. Pleasance ED, Stephens PJ, O'Meara S, McBride DJ, Meynert A, Jones D, et al.A small-cell lung cancer genome with complex signatures of tobacco exposure. Nature2010;463:184–90. [PubMed: 20016488]
10. Poon SL, Pang ST, McPherson JR, Yu W, Huang KK, Guan P, et al.Genome-wide mutational signatures of aristolochic acid and its application as a screening tool. Sci Transl Med2013;5:197ra01.
11. van Thuijl HF, Mazor T, Johnson BE, Fouse SD, Aihara K, Hong C, et al.Evolution of DNA repair defects during malignant progression of low-grade gliomas after temozolomide treatment. Acta Neuropathol2015;129:597–607. [PubMed: 25724300]
12. Loeb LA, Springgate CF, Battula N. Errors in DNA replication as a basis of malignant changes. Cancer Res1974;34:2311–21. [PubMed: 4136142]
13. Tomasetti C, Li L, Vogelstein B. Stem cell divisions, somatic mutations, cancer etiology, and cancer prevention. Science2017;355:1330–4. [PubMed: 28336671]
14. Palles C, Cazier JB, Howarth KM, Domingo E, Jones AM, Broderick P, et al.Germline mutations affecting the proofreading domains of POLE and POLD1 predispose to colorectal adenomas and carcinomas. Nat Genet2013;45:136–44. [PubMed: 23263490]
15. Bonadona V, Bonaiti B, Olschwang S, Grandjouan S, Huiart L, Longy M, et al.Cancer risks associated with germline mutations in MLH1, MSH2, and MSH6 genes in Lynch syndrome. JAMA2011;305:2304–10. [PubMed: 21642682]
16. Shlien A, Campbell BB, de Borja R, Alexandrov LB, Merico D, Wedge D, et al.Combined hereditary and somatic mutations of replication error repair genes result in rapid onset of ultra-hypermutated cancers. Nat Genet2015;47:257–62. [PubMed: 25642631]
17. Johanns TM, Miller CA, Dorward IG, Tsien C, Chang E, Perry A, et al.Immunogenomics of hypermutated glioblastoma: a patient with germline POLE deficiency treated with checkpoint blockade immunotherapy. Cancer Discov2016;6:1230–6. [PubMed: 27683556]
18. Bouffet E, Larouche V, Campbell BB, Merico D, de Borja R, Aronson M, et al.Immune checkpoint inhibition for hypermutant glioblastoma multiforme resulting from germline biallelic mismatch repair deficiency. J Clin Oncol2016;34:2206–11. [PubMed: 27001570]
19. Errico A. Melanoma: CheckMate 067–frontline nivolumab improves PFS alone or in combination with ipilimumab. Nat Rev Clin Oncol2015;12:435. [PubMed: 26099982]

20. Rizvi NA, Hellmann MD, Snyder A, Kvistborg P, Makarov V, Havel JJ, et al.Mutational landscape determines sensitivity to PD-1 blockade in non-small cell lung cancer. Science2015;348:124–8. [PubMed: 25765070]
21. Santin AD, Bellone S, Buza N, Choi J, Schwartz PE, Schlessinger J, et al.Regression of chemotherapy-resistant polymerase epsilon (POLE) ultra-mutated and MSH6 hyper-mutated endometrial tumors with nivolumab. Clin Cancer Res2016;22:5682–7. [PubMed: 27486176]
22. Le DT, Uram JN, Wang H, Bartlett BR, Kemberling H, Eyring AD, et al.PD-1 blockade in tumors with mismatch-repair deficiency. N Engl J Med2015;372:2509–20. [PubMed: 26028255]
23. Vandeven N, Lewis CW, Makarov V, Riaz N, Paulson KG, Hippe D, et al.Merkel cell carcinoma patients presenting without a primary lesion have elevated markers of immunity, higher tumor mutation burden, and improved survival. Clin Cancer Res2018;24:963–71. [PubMed: 29246939]
24. Overman MJ, McDermott R, Leach JL, Lonardi S, Lenz HJ, Morse MA, et al.Nivolumab in patients with metastatic DNA mismatch repair-deficient or microsatellite instability-high colorectal cancer (CheckMate 142): an open-label, multicentre, phase 2 study. Lancet Oncol2017;18:1182–91. [PubMed: 28734759]
25. Marabelle A, Le DT, Ascierto PA, Giacomo AMD, Jesus-Acosta AD, Delord J-P, et al.Efficacy of pembrolizumab in patients with noncolorectal high microsatellite instability/mismatch repair–deficient cancer: results from the phase II KEYNOTE-158 study. J Clin Oncol2020;38:1–10. [PubMed: 31682550]
26. Le DT, Kim TW, Cutsem EV, Geva R, Jäger D, Hara H, et al.Phase II open-label study of pembrolizumab in treatment-refractory, microsatellite instability–high/mismatch repair–deficient metastatic colorectal cancer: KEYNOTE-164. J Clin Oncol2020;38:11–9. [PubMed: 31725351]
27. Overman MJ, Lonardi S, Wong KYM, Lenz H-J, Gelsomino F, Aglietta M, et al.Durable clinical benefit with nivolumab plus ipilimumab in DNA mismatch repair–deficient/microsatellite instability–high metastatic colorectal cancer. J Clin Oncol2018;36:773–9. [PubMed: 29355075]
28. Montagut C, Settleman J. Targeting the RAF-MEK-ERK pathway in cancer therapy. Cancer Lett2009;283:125–34. [PubMed: 19217204]
29. Sebolt-Leopold JS, Herrera R. Targeting the mitogen-activated protein kinase cascade to treat cancer. Nat Rev Cancer2004;4:937–47. [PubMed: 15573115]
30. Martincorena I, Raine KM, Gerstung M, Dawson KJ, Haase K, Van Loo P, et al.Universal patterns of selection in cancer and somatic tissues. Cell2017;171:1029–41. [PubMed: 29056346]
31. Chang MT, Bhattarai TS, Schram AM, Bielski CM, Donoghue MTA, Jonsson P, et al.Accelerating discovery of functional mutant alleles in cancer. Cancer Discov2018;8:174–83. [PubMed: 29247016]
32. Frampton GM, Fichtenholtz A, Otto GA, Wang K, Downing SR, He J, et al.Development and validation of a clinical cancer genomic profiling test based on massively parallel DNA sequencing. Nat Biotechnol2013;31:1023–31. [PubMed: 24142049]
33. Durno CA, Sherman PM, Aronson M, Malkin D, Hawkins C, Bakry D, et al.Phenotypic and genotypic characterisation of biallelic mismatch repair deficiency (BMMR-D) syndrome. Eur J Cancer2015;51:977–83. [PubMed: 25883011]
34. Eleveld TF, Oldridge DA, Bernard V, Koster J, Daage LC, Diskin SJ, et al.Relapsed neuroblastomas show frequent RAS-MAPK pathway mutations. Nat Genet2015;47:864–71. [PubMed: 26121087]
35. Schubert M, Klinger B, Klünemann M, Sieber A, Uhlitz F, Sauer S, et al.Perturbation-response genes reveal signaling footprints in cancer gene expression. Nat Commun2018;9:20. [PubMed: 29295995]
36. Dry JR, Pavey S, Pratilas CA, Harbron C, Runswick S, Hodgson D, et al.Transcriptional pathway signatures predict MEK addiction and response to selumetinib (AZD6244). Cancer Res2010;70:2264–73. [PubMed: 20215513]
37. Liberzon A, Birger C, Thorvaldsdóttir H, Ghandi M, Mesirov Jill P, Tamayo P. The molecular signatures database hallmark gene set collection. Cell Syst2015;1:417–25. [PubMed: 26771021]
38. Yaeger R, Yao Z, Hyman DM, Hechtman JF, Vakiani E, Zhao H, et al.Mechanisms of acquired resistance to BRAF V600E inhibition in colon cancers converge on RAF dimerization and are sensitive to its inhibition. Cancer Res2017;77:6513–23. [PubMed: 28951457]

39. Shannon S, Jia D, Entersz I, Beelen P, Yu M, Carcione C, et al.Inhibition of glioblastoma dispersal by the MEK inhibitor PD0325901. BMC Cancer2017;17:121. [PubMed: 28187762]
40. Canale FP, Ramello MC, Núñez N, Araujo Furlan CL, Bossio SN, Gorosito Serrán M, et al.CD39 expression defines cell exhaustion in tumor-infiltrating CD8(+) T cells. Cancer Res2018;78:115–28. [PubMed: 29066514]
41. Duhen T, Duhen R, Montler R, Moses J, Moudgil T, de Miranda NF, et al.Co-expression of CD39 and CD103 identifies tumor-reactive CD8 T cells in human solid tumors. Nat Commun2018;9:2724. [PubMed: 30006565]
42. D'Angelo F, Ceccarelli M, Tala Garofano L, Zhang J, Frattini V, et al.The molecular landscape of glioma in patients with neurofibromatosis 1. Nat Med2019;25:176–87. [PubMed: 30531922]
43. Zehir A, Benayed R, Shah RH, Syed A, Middha S, Kim HR, et al.Mutational landscape of metastatic cancer revealed from prospective clinical sequencing of 10,000 patients. Nat Med2017;23:703–13. [PubMed: 28481359]
44. Oshrine B, Grana N, Moore C, Nguyen J, Crenshaw M, Edwards M, et al.B-cell acute lymphoblastic leukemia with high mutation burden presenting in a child with constitutional mismatch repair deficiency. Blood Adv2019;3:1795–8. [PubMed: 31189528]
45. Sun C, Fang Y, Yin J, Chen J, Ju Z, Zhang D, et al.Rational combination therapy with PARP and MEK inhibitors capitalizes on therapeutic liabilities in RAS mutant cancers. Sci Transl Med2017;9:eaal5148.
46. Maertens O, Kuzmickas R, Manchester HE, Emerson CE, Gavin AG, Guild CJ, et al.MAPK pathway suppression unmasks latent DNA repair defects and confers a chemical synthetic vulnerability in BRAF-, NRAS-, and NF1-mutant melanomas. Cancer Discov2019;9: 526–45. [PubMed: 30709805]
47. Hellmann MD, Ciuleanu TE, Pluzanski A, Lee JS, Otterson GA, Audigier-Valette C, et al.Nivolumab plus ipilimumab in lung cancer with a high tumor mutational burden. N Engl J Med2018;378:2093–104. [PubMed: 29658845]
48. Sharma P, Allison JP. Immune checkpoint targeting in cancer therapy: toward combination strategies with curative potential. Cell2015; 161:205–14. [PubMed: 25860605]
49. Mahoney KM, Freeman GJ, McDermott DF. The next immune-checkpoint inhibitors: PD-1/PD-L1 blockade in melanoma. Clin Ther2015;37:764–82. [PubMed: 25823918]
50. Kyi C, Postow MA. Immune checkpoint inhibitor combinations in solid tumors: opportunities and challenges. Immunotherapy2016; 8:821–37. [PubMed: 27349981]
51. Hellmann MD, Kim TW, Lee CB, Goh BC, Miller WH Jr, Oh DY, et al.Phase Ib study of atezolizumab combined with cobimetinib in patients with solid tumors. Ann Oncol2019;30:1134–42. [PubMed: 30918950]
52. Eng C, Kim TW, Bendell J, Argilés G, Tebbutt NC, Di Bartolomeo M, et al.Atezolizumab with or without cobimetinib versus regorafenib in previously treated metastatic colorectal cancer (IMblaze370): a multicentre, open-label, phase 3, randomised, controlled trial. Lancet Oncol2019;20:849–61. [PubMed: 31003911]
53. Miller CA, White BS, Dees ND, Griffith M, Welch JS, Griffith OL, et al.SciClone: inferring clonal architecture and tracking the spatial and temporal patterns of tumor evolution. PLoS Comput Biol2014;10:e1003665.
54. Adzhubei I, Jordan DM, Sunyaev SR. Predicting functional effect of human missense mutations using PolyPhen-2. Curr Protoc Hum Genet2013;76:7.20.1–7.41.
55. Fedele C, Ran H, Diskin B, Wei W, Jen J, Geer MJ, et al.SHP2 inhibition prevents adaptive resistance to MEK inhibitors in multiple cancer models. Cancer Discov2018;8:1237–49. [PubMed: 30045908]
56. Lin L, Sabnis AJ, Chan E, Olivas V, Cade L, Pazarentzos E, et al.The Hippo effector YAP promotes resistance to RAF- and MEK-targeted cancer therapies. Nat Genet2015;47:250–6. [PubMed: 25665005]
57. Yao Z, Yaeger R, Rodrik-Outmezguine VS, Tao A, Torres NM, Chang MT, et al.Tumours with class 3 BRAF mutants are sensitive to the inhibition of activated RAS. Nature2017;548:234–8. [PubMed: 28783719]

58. Lin GL, Wilson KM, Ceribelli M, Stanton BZ, Woo PJ, Kreimer S, et al.Therapeutic strategies for diffuse midline glioma from high-throughput combination drug screening. Sci Transl Med2019;11:eaaw0064.

59. Bartholomeusz C, Oishi T, Saso H, Akar U, Liu P, Kondo K, et al.MEK1/2 inhibitor selumetinib (AZD6244) inhibits growth of ovarian clear cell carcinoma in a PEA-15-dependent manner in a mouse xenograft model. Mol Cancer Ther2012;11:360–9. [PubMed: 22144664]

60. Troiani T, Vecchione L, Martinelli E, Capasso A, Costantino S, Ciuffreda LP, et al.Intrinsic resistance to selumetinib, a selective inhibitor of MEK1/2, by cAMP-dependent protein kinase A activation in human lung and colorectal cancer cells. Br J Cancer2012;106: 1648–59. [PubMed: 22569000]

SIGNIFICANCE:

Tumors harboring a single *RAS/MAPK* driver mutation are targeted individually for therapeutic purposes. We find that in RRD hypermutant cancers, mutations in the RAS/MAPK pathway are enriched, highly expressed, and result in sensitivity to MEK inhibitors. Targeting an oncogenic pathway may provide therapeutic options for these hypermutant polyclonal cancers.

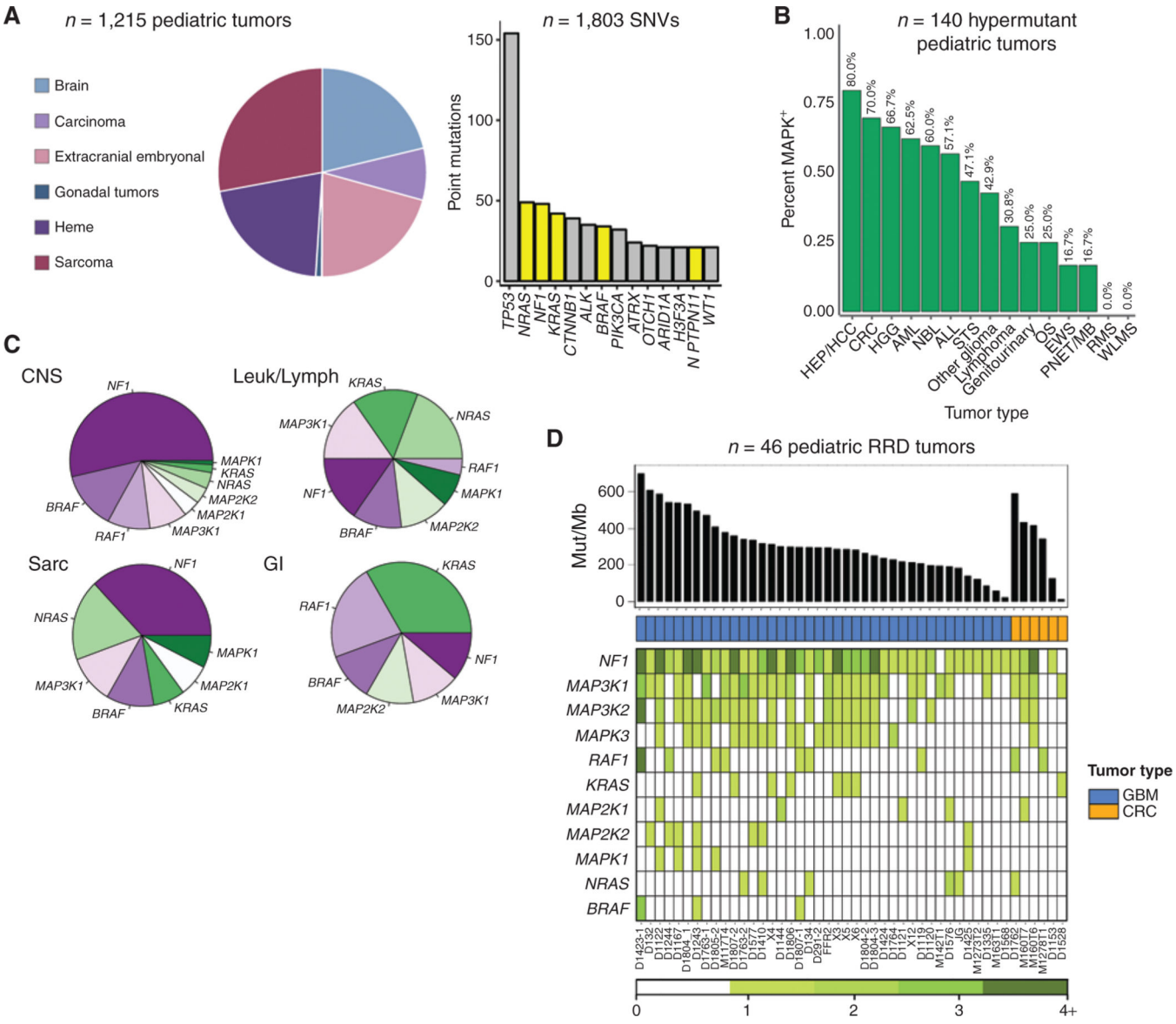

Figure 1.

Prevalence of RAS/MAPK genetic events across 1,215 pediatric cancers. **A,** Pie graph indicates the tissue of origin of 1,215 pediatric cancers. 1,803 SNVs were detected across the entire cohort; RAS/MAPK-activating events are indicated in yellow. **B,** Prevalence of RAS/MAPK mutations in hypermutant pediatric tumors, stratified by tumor type. HEP/HCC, hepatocellular carcinoma; CRC, colorectal cancer; HGG, high grade glioma; AML, acute myeloid leukemia; NBL, neuroblastoma; ALL, acute lymphocytic leukemia; STS, soft tissue sarcoma; OS, osteosarcoma; EWS, Ewing sarcoma; PNET/MB, primitive neuroectodermal tumors/medulloblastoma; RMS, rhabdomyosarcoma; WLMS, Wilms tumor. **C,** Pie graphs demonstrating the distribution of the 11 most commonly mutated RAS/MAPK genes across different tissues of origin. **D,** Exome sequencing of 46 glioblastomas (GBM) and colorectal cancers (CRC) from patients with germline mutations in MMR and

POLE. Top, tumor mutation burden in mutations/mb; middle, tumor type and number of nonsynonymous, protein-coding events in 11 commonly mutated RAS/MAPK genes.

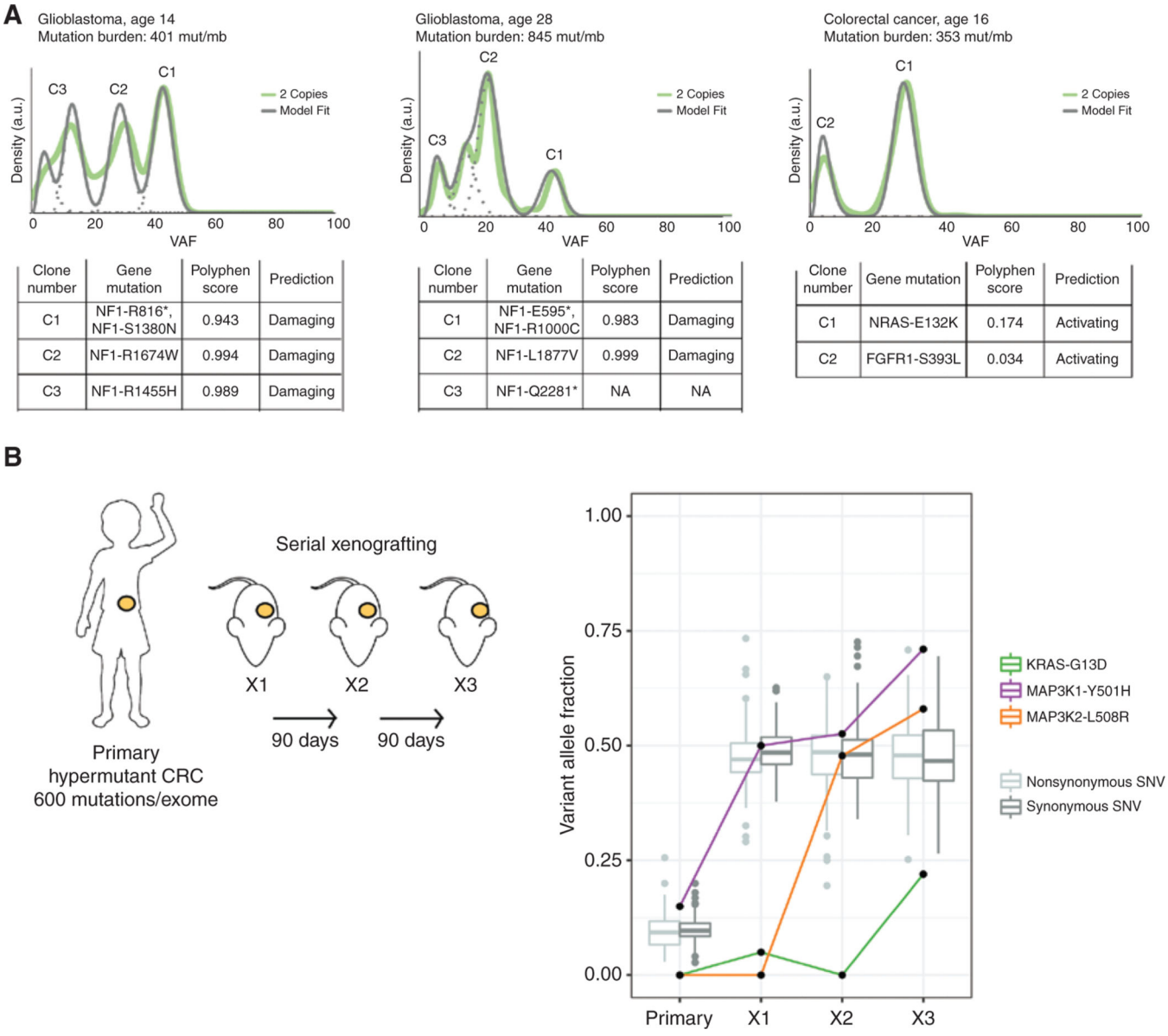

Clone number	Gene mutation	Polyphen score	Prediction
C1	NF1-R816*, NF1-S1380N	0.943	Damaging
C2	NF1-R1674W	0.994	Damaging
C3	NF1-R1455H	0.989	Damaging

Clone number	Gene mutation	Polyphen score	Prediction
C1	NF1-E595*, NF1-R1000C	0.983	Damaging
C2	NF1-L1877V	0.999	Damaging
C3	NF1-Q2281*	NA	NA

Clone number	Gene mutation	Polyphen score	Prediction
C1	NRAS-E132K	0.174	Activating
C2	FGFR1-S393L	0.034	Activating

Figure 2.

Prevalence of RAS/MAPK mutations in polyclonal and temporal sampling of RRD tumors. **A,** Clonal analysis of three heavily mutated tumors and the respective RAS/MAPK mutations in each clone. PolyPhen scores for each mutation distinguish damaging mutations in negative regulators, in contrast to benign or activating mutations in gain-of-function genes **B,** Schematic of serial xenografting experiment performed on one hypermutant patient-derived colorectal cancer (CRC) xenograft (left). Changes in the VAF of RAS/MAPK genes mutated in the primary and subsequent xenografts. All mutations increase in tumor fraction, suggesting positive selection, whereas other variants in the primary remain stable (right).

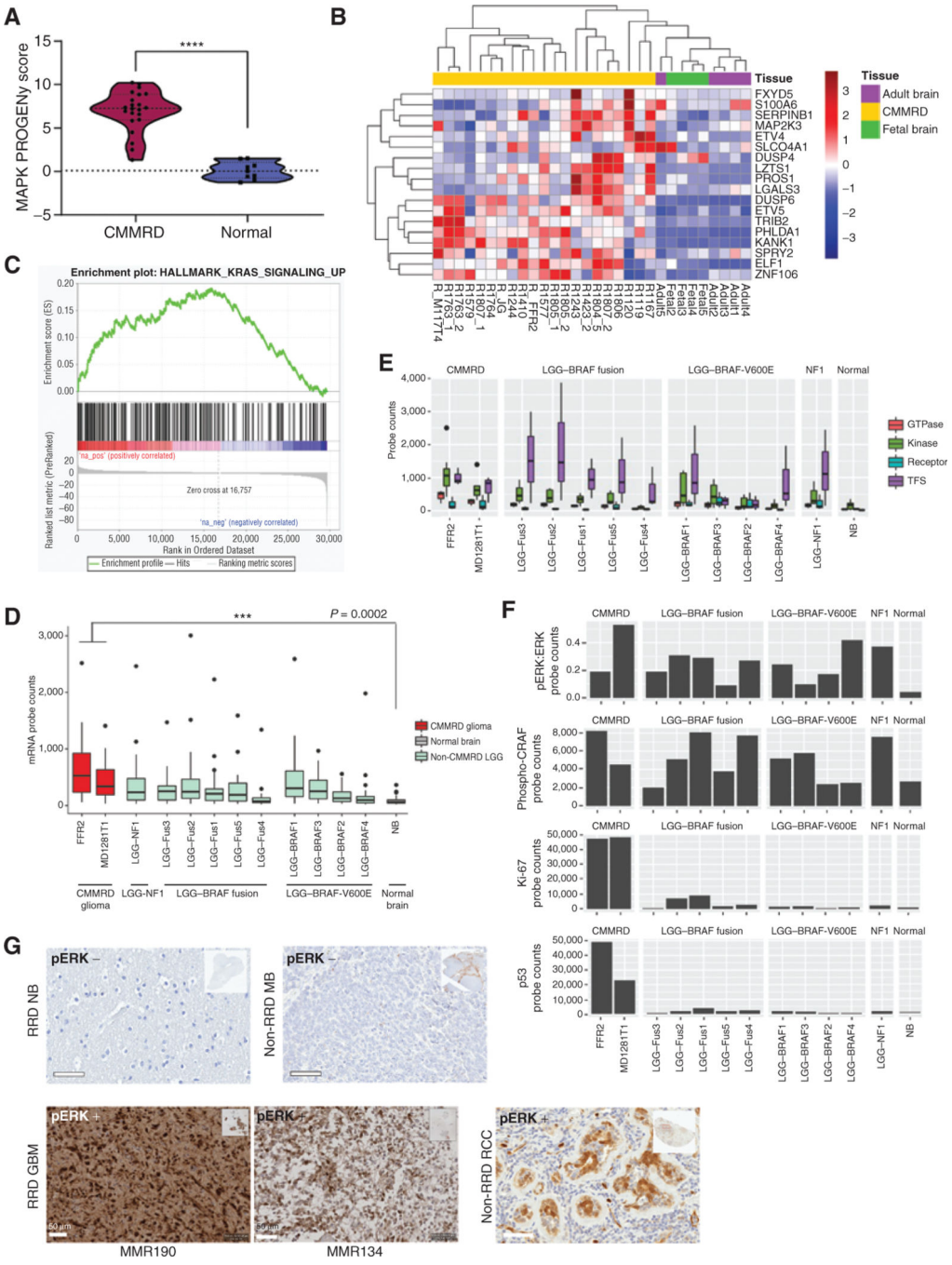

Figure 3.

Assessment of RAS/MAPK pathway activation in hypermutant RRD gliomas. **A,** Violin plot of RNA-seq–derived MAPK pathway PROGENy signature scores of CMMRD GBMs ($n = 21$) compared with normal fetal ($n = 4$) and adult ($n = 5$) brains ($P < 0.0001$; Welch t test). Lines indicate median and quartile values. **B,** Unsupervised clustering of all samples in **A** based on expression of an 18-gene RAS transcriptional output signature. **C,** GSEA enrichment plot for genes upregulated by KRAS activation in CMMRD GBM vs. normal brain samples in **A** and **B.** NES is reported (FDR = 0). **D,** NanoString counts

of single mRNA molecules in 20 RAS/MAPK pathway–related probes, including *EGFR, BRAF, KRAS, MAP3K1, FOS*, and *JUN*, in CMMRD GBM compared with tissue-matched *BRAF*^{V600E} mutant low-grade gliomas. **E,** NanoString counts of single mRNA molecules in 20 RAS/MAPK pathway–related probes, stratified by protein-type. Transcription factor targets of the RAS/MAPK pathway were the most upregulated. **F,** NanoString counts of single protein molecules involved in RAS/MAPK pathway activation, including phospho-ERK and phospho-CRAF. Ki-67 protein levels are shown to highlight the distinguishing growth characteristics of LGG versus GBM. For box plots **D–E,** median and quartile values are depicted. **G,** Positive IHC staining for phospho-ERK (pERK) on two representative CMMRD brain tumors harboring several RAS/MAPK pathway alterations (bottom left; MMR190 and MMR134), compared with a CMMRD normal postmortem brain sample and non-RRD pediatric medulloblastoma demonstrating negative staining (top), and a human renal cell carcinoma (RCC) sample demonstrating nuclear and cytoplasmic staining of phospho-ERK in tubular epithelial structures surrounded by negatively staining lymphocytes (bottom right). Scale bars, 50 μm. ****, $P < 0.0001$.

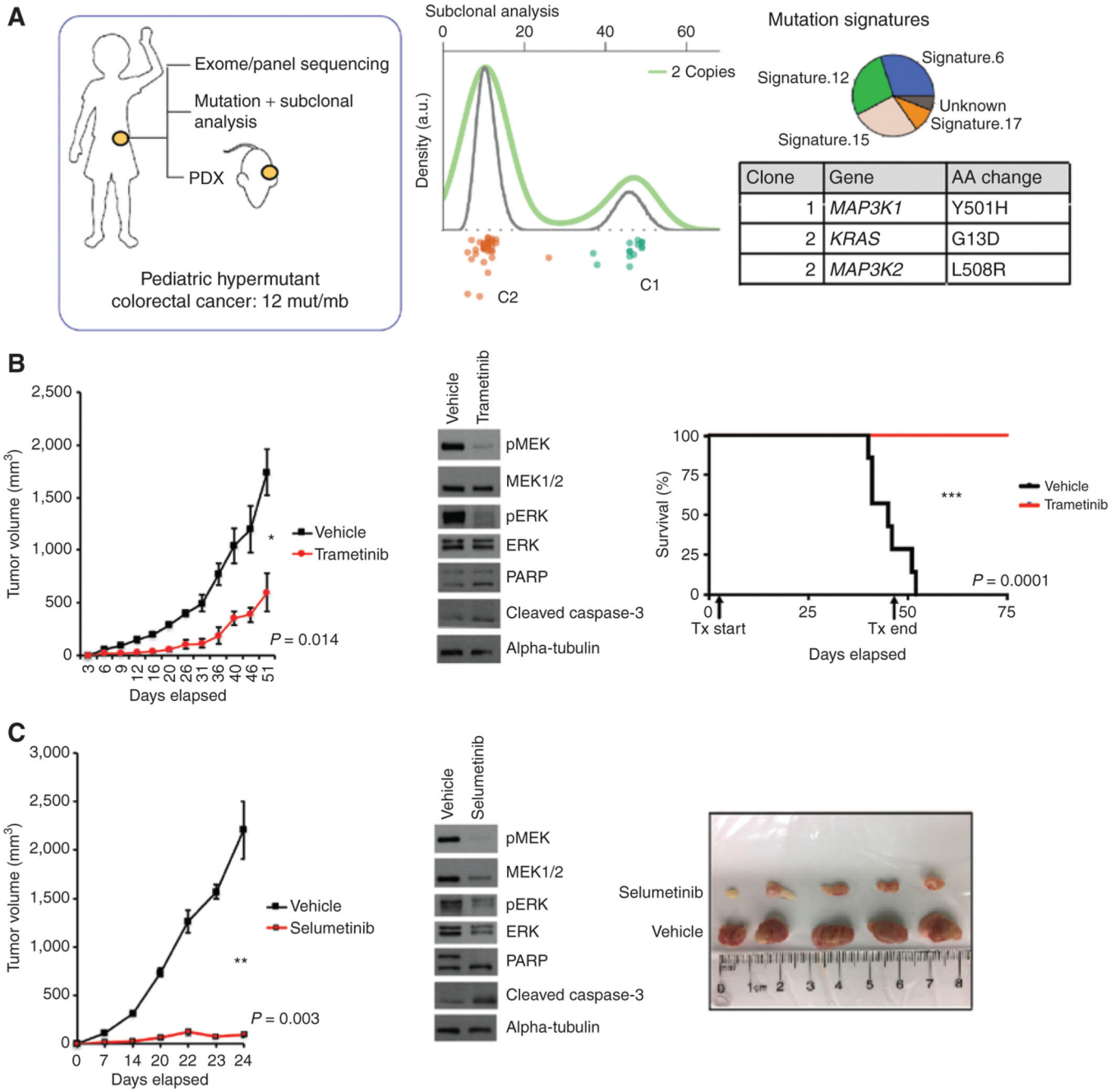

Figure 4.

Genomic characterization and subsequent xenografting and treatment of an ultrahypermutant childhood colorectal cancer. **A,** Schematic of tumor sequencing analysis performed on a patient-derived hypermutant colorectal cancer. Targeted panel sequencing revealed two major clones. A secondary *KRAS*^{G13D} known RAS/MAPK driver pathway mutation was acquired in the secondary clone. Mutation signatures within the tumor reveal a characteristic pattern of RRD. **B,** Tumor growth experiments in response to MEK inhibition therapy (trametinib) for flank-implanted colorectal cancer xenograft. Tumor volume was measured biweekly in trametinib treated vs. vehicle group. Western blot analysis of tissues and the

conclusion of the experiment reveal a decrease in phospho-MEK and phospho-ERK. A second repeated experiment to demonstrate survival differences is shown. **C,** Tumor growth experiments in response to MEK inhibition therapy using selumetinib. Mice were sacrificed after 24 days to display differences in tumor sizes.

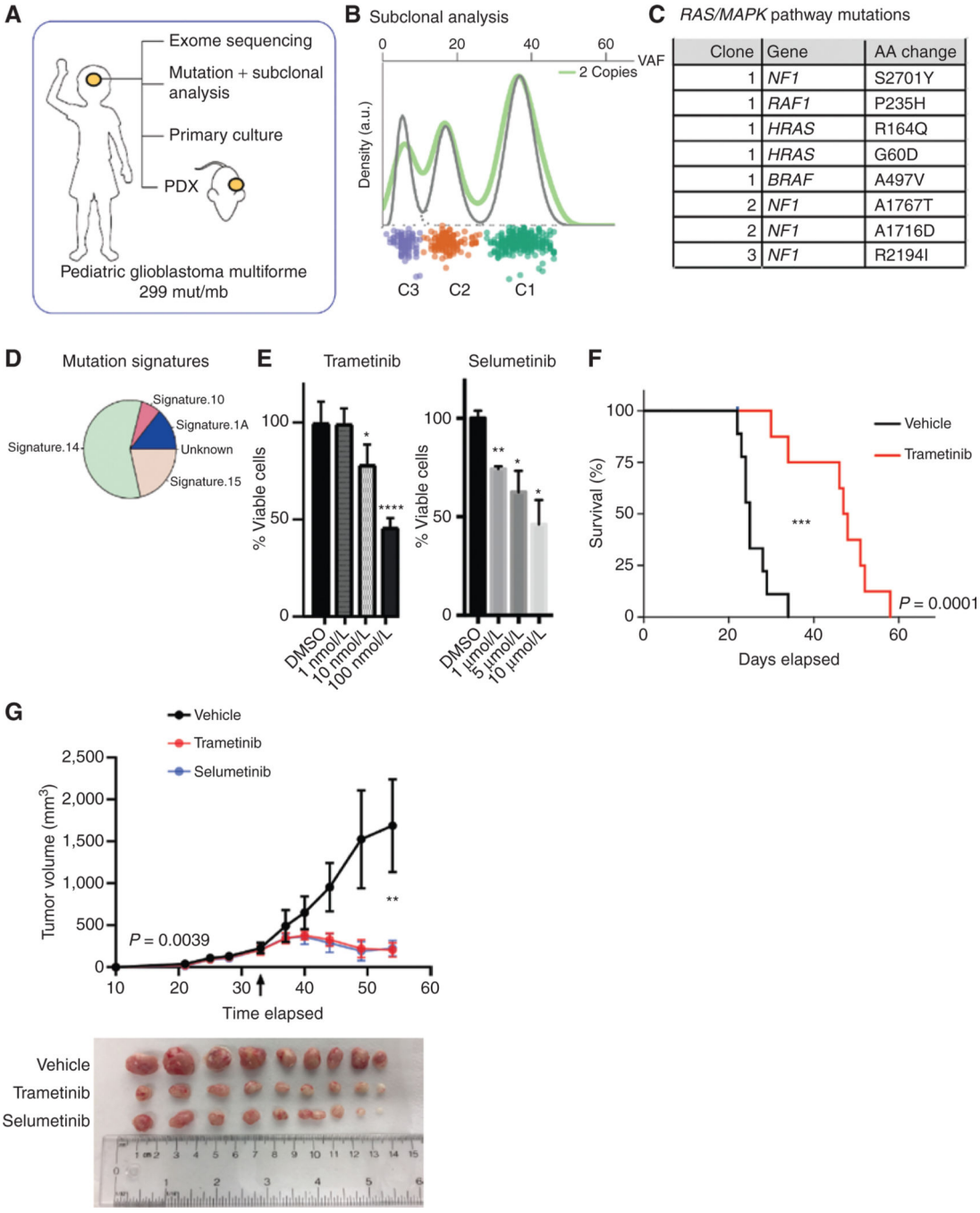

Figure 5.

Genomic characterization and subsequent xenografting and treatment of an ultrahypermutant childhood glioblastoma. **A,** Schematic of experiments performed on a CMMRD pediatric glioblastoma. **B,** Subclonal analysis reveals multiple mutations per clone. **C,** Identity of RAS/MAPK pathway–related alterations in this tumor. **D,** Mutational signature analysis reveals the source of mutations as RRD. **E,** Primary culturing of cells derived from this tumor, without prior culturing, and treatment with either trametinib or selumetinib. **F,** Survival experiment following flank implantation of this ultrahypermutant GBM and

subsequent treatment *in vivo* with trametinib. **G,** A second set of flank engraftment experiments were conducted to assess tumor growth following flank implantation and treatment with trametinib or selumetinib. Arrow indicates time at which treatment commenced.

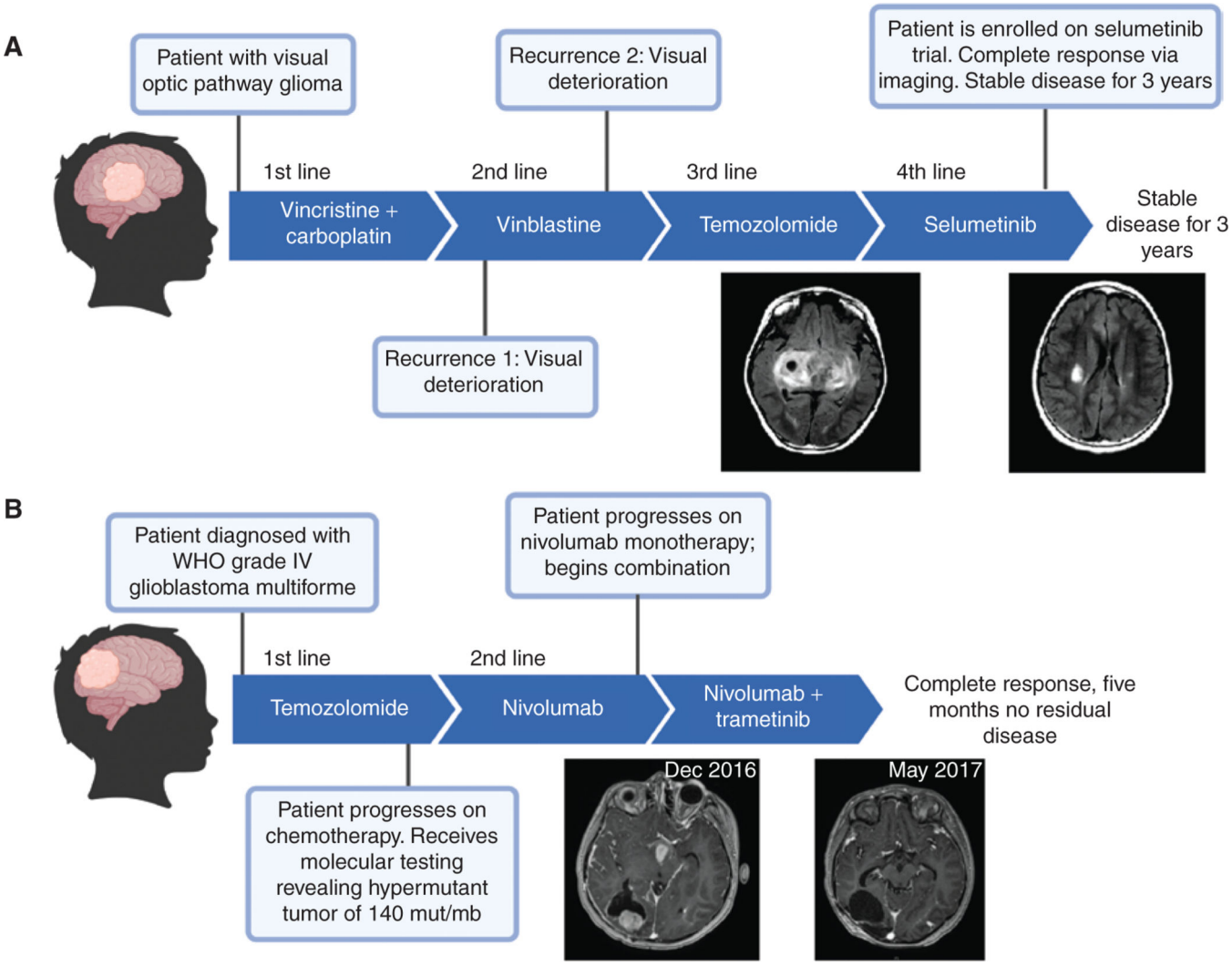

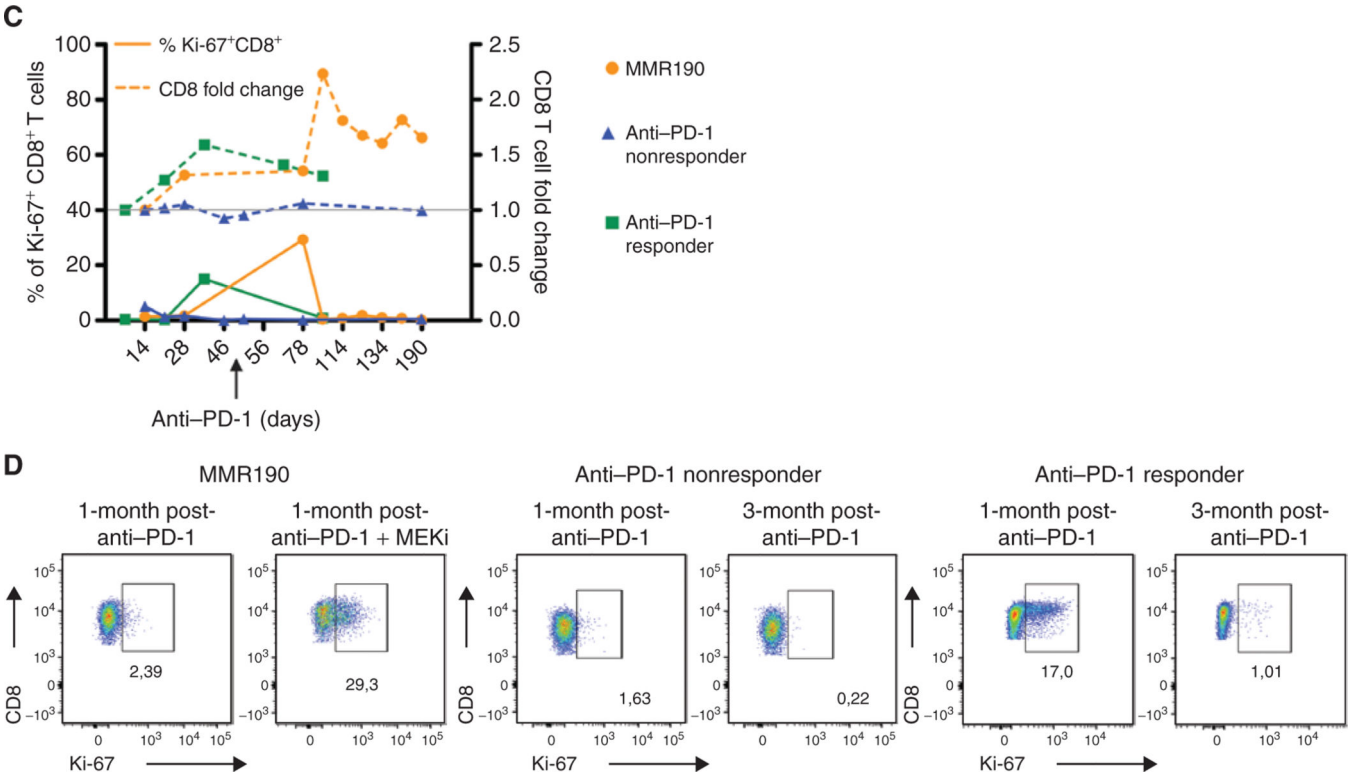

Figure 6.

Clinical response of patients with replication repair–deficient high-grade gliomas to MEK inhibitors. Previous failed treatment courses and sustained responses to selumetinib **(A)** and trametinib **(B)**, respectively. **C,** Correlation between immune activation and clinical response to MEK inhibition in patient 2 (MMR190). Percentage of $CD3^+CD8^+$ PBMCs expressing Ki-67 (left axis) and fold change in total $CD3^+CD8^+$ PBMCs (right axis) over time in patients with GBM tumors that showed response to anti–PD-1 monotherapy, no response to anti–PD-1 monotherapy, and response to combination anti–PD-1 and the MEK inhibitor trametinib (MMR190—patient 2 from 6B). Arrow indicates start of trametinib administration. **D,** Ki-67 expression on $CD3^+CD8^+$ PBMCs one month following anti–PD-1 treatment initiation, and one month following combination anti–PD-1/MEK inhibition (MMR190) or three months following anti–PD-1 initiation (anti–PD-1 responder and nonresponder). MEKi = trametinib.